


Many-Body Effects in Strongly Disordered III-Nitride Quantum Wells: Interplay Between Carrier Localization and Coulomb Interaction

Aurelien David,^{*} Nathan G. Young, and Michael D. Craven
Soraa Inc., 6500 Kaiser Dr., Fremont, California 94555, USA

 (Received 8 April 2019; revised manuscript received 7 August 2019; published 25 October 2019)

The joint impact of Anderson localization and many-body interaction is observed in the optical properties of strongly disordered III-nitride quantum wells, a system where the Coulomb interaction and the fluctuating potential are pronounced effects with similar magnitude. A numerical method is introduced to solve the six-dimensional coupled Schrodinger equation in the presence of disorder and Coulomb interaction, a challenging numerical task. It accurately reproduces the measured absorption and luminescence dynamics of (In,Ga)N quantum wells at room-temperature: absorption spectra reveal the existence of a broadened excitonic peak, and carrier lifetime measurements show that luminescence departs from a conventional bimolecular behavior. These results reveal that luminescence is governed by the interplay between localization and Coulomb interaction, and provide practical insight into the physics of modern light-emitting diodes.

DOI: [10.1103/PhysRevApplied.12.044059](https://doi.org/10.1103/PhysRevApplied.12.044059)

I. INTRODUCTION

The physics of compound semiconductors is influenced by many-body interaction as well as disorder. In conventional semiconductors, disorder effects are weak compared to the Coulomb interaction, and disorder can be treated as a perturbation to the excitonic center of mass. This has led to multiple signatures at cryogenic temperatures in the widely studied system of GaAs/(Al,Ga)As quantum wells (QWs) with disordered interfaces, using absorption and luminescence as probes for the quantum state of the system [1–9].

More recently, the mastery of III-nitride compounds—the material system of choice for modern light-emitting diodes (LEDs)—has renewed interest in the physics of luminescence of disordered semiconductors by giving access to a new physical regime. Indeed, these materials constitute a remarkable system where the two effects are strongly pronounced: Coulomb interaction leads to an excitonic binding energy of tens of meVs, with an associated Bohr radius of a few nm; meanwhile, Anderson localization of carriers stems from inherent random alloy disorder, with fluctuations in potential energy of approximately 100 meV and typical dimensions of a few nm. Therefore, both phenomena occur with a similar scale of energy (large enough to be relevant at room temperature) and distance, and must be considered on equal footing rather than perturbatively. III-nitride QWs thus offer an

ideal testbed to study the unique regime of strong disorder with strong Coulomb interaction, with the practical perspective of better understanding the fundamental limits of this material for LED applications.

Recent experimental work has shown evidence of localization effects in III-nitride QWs [10–13] with signatures reminiscent of that in conventional semiconductors [2–6,14]; on the other hand, direct observation of Coulomb-interaction effects has been elusive (apart from signatures at cryogenic temperature in *m*-plane samples [15,16]). From a theoretical standpoint, alloy disorder [17–21] and many-body effects [22,23] have been investigated independently. Their joint consideration is a more complex task; it was first tackled recently in Refs. [18] and [24], with the limitation that the Coulomb-interacting problem is solved over a basis of a few free-carrier eigenstates. Overall, these theoretical investigations predict corrections of the radiative rate of about 10%–30% compared to disorder-free models; these have not been validated experimentally.

In this Letter, we present direct experimental evidence of the effects of localization and many-body interaction on the room-temperature optical properties of high-quality (In,Ga)N QWs, and show that their magnitude well exceeds the aforementioned predictions. We introduce an advanced numerical model, which treats these on equal footing by solving the full six-dimensional Schrodinger equation. This approach quantitatively reproduces experimental results, confirming that the interplay between the two effects is essential in understanding III-nitride luminescence and the resulting LED efficiency.

^{*} aurelien.david@polytechnique.org

II. ABSORPTION

We begin by investigating the absorption coefficient (α) in (In,Ga)N QWs, since excitonic effects are commonly manifested by sharp absorption peaks. Such peaks are indeed observed in bulk GaN samples at cryogenic temperature [25]. In contrast, measurements on QWs usually result in broad spectra, which lack excitonic signatures. We illustrate this using a sample, grown on a bulk GaN substrate by metalorganic chemical vapor deposition, having a 3.5-nm-thick (In,Ga)N QW with [In] = 13% placed at the center of a *p-i-n* junction. Its room-temperature absorption, measured by photocurrent spectroscopy [11,26], lacks distinct features, as shown in Fig. 1(a).

Such featureless absorption is attributed to the inhomogeneous broadening caused by the strong polarization field present across the QW, and to the reduction in Coulomb interaction due to electron-hole wave function separation. To remove these effects, we perform photocurrent measurements under reverse bias to compensate for the polarization field. As the bias is varied, the absorption spectrum progressively sharpens until the QW reaches flat-band conditions [Fig. 1(a)], where an excitonic peak is observed [27]. We systematically observe similar spectra in other samples of varying QW design (as already reported in Ref. [27]). This excitonic peak constitutes a rare direct manifestation of many-body effects at room temperature in (In,Ga)N QWs, and offers an opportunity to validate theoretical models.

We now present a numerical model, which predicts such optical features by taking into account alloy disorder and Coulomb interaction. Since both effects are of similar magnitude, they cannot be treated perturbatively as has been done in other material systems. We place ourselves in the two-band effective mass approximation; this is appropriate to describe the near-band-edge optical behavior. The

electron-hole Hamiltonian reads

$$H_r = -\frac{\hbar^2}{2m_e}\Delta_e + V_e - \frac{\hbar^2}{2m_h}\Delta_h + V_h + V_C. \quad (1)$$

Here $\Delta_{e,h}$ are the Laplacian operators on the electron and hole coordinates, $V_{e,h}$ the electrostatic potentials for the electron and hole (including alloy disorder), and V_C the Coulomb interaction term.

Because it includes disorder and Coulomb interaction, Eq. (1) is a six-dimensional problem (three dimensions per carrier, coupled together), making it very challenging numerically. The standard approach (summing optical transitions over eigenstates of H_r) is prohibitive as several thousand eigenstates are required for a proper description of the optical joint density of states (JDOS). Instead, we proceed by solution of the time-dependent Schrodinger equation in real space, following the general approach of Refs. [28] and [29]. In short, the optical polarization is propagated in time, which directly yields the JDOS and absorption without requiring eigenstates. This makes the method computationally efficient, although it has not previously been applied to problems with such complexity. We mention important aspects of the model below; implementation details are in the Supplemental Material (SM) [30].

The Hamiltonian is discretized in real space with a standard finite-difference scheme. To account for alloy disorder in $V_{e,h}$, we create smoothed numerical maps of atomic potentials following the approach of Refs. [11] and [17]. Unlike other published works, we do not assume thickness fluctuations (careful atom force microscopy studies did not reveal their presence in our samples).

The Coulomb term V_C deserves caution. Since $V_C \sim 1/r$, a naive discretization diverges at $r = 0$, causing well-known numerical difficulties. The often-proposed simple regularization $V_C \sim 1/(r^2 + a^2)^{1/2}$ (with a an empiri-

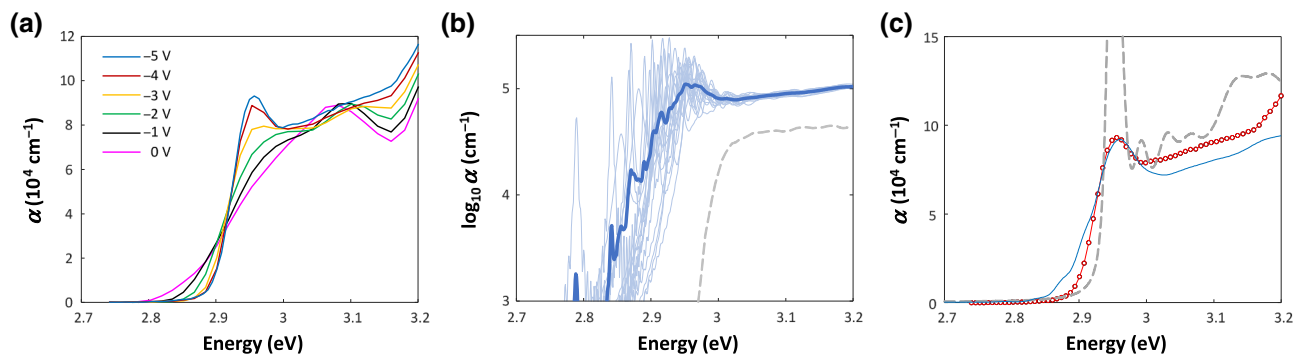


FIG. 1. Absorption properties of a 3.5-nm-thick (In,Ga)N QW. (a) α measured by photocurrent at various reverse biases, showing the progressive appearance of an excitonic resonance. (b) Modeled α (in log scale) in flat-band conditions. Thin lines, individual configurations. Thick line, average of 40 calculations. Dashed line, average without Coulomb interaction, for comparison. (c) Comparison of measured (solid line with dots) and modeled (solid line) α , showing excellent agreement. Dashed line, modeled α without disorder.

cal short-scale constant) suffers from poor convergence. Instead, we investigate two more sophisticated approaches: the so-called ground-state scheme [28,29] and asymptotic-behavior-correspondence (ABC) scheme [31]. Both lead to near-identical results in our simulations. As we will see hereafter, the model ultimately needs to account for carrier-screening effects. Therefore, we select the ABC scheme because it can straightforwardly be generalized to arbitrary carrier populations [32]. The Coulomb term thus reads $V_C = -e^2/4\pi\epsilon\bar{r}$, with \bar{r} the effective radius derived from the ABC scheme and ϵ the dielectric constant of GaN.

With this model, we compute the optical absorption of a QW in flat-band conditions. Figure 1(b) shows several calculations with different configurations of the alloy distribution, and the average of 40 calculations. For each configuration, sharp excitonic peaks are observed. Near the band edge these peaks are dense; each configuration also displays a few deeply localized excitonic peaks: these correspond to excitonic states stemming from Anderson-localized holes at random In-rich locations in the QW. These deep states produce an Urbach tail for the average absorption, with a characteristic energy approximately 20 meV, similar to the measurements of Ref. [11]. Note that ignoring Coulomb interaction would lead to a narrower Urbach tail [7 meV, Fig. 1(b)]. The Urbach tail is often considered as a manifestation of wave function localization [14,33]; our results show that Coulomb interaction further affects its behavior. We infer that the observed increase in Urbach energy is caused by a more pronounced Coulomb interaction among deeply localized states.

Figure 1(c) compares the average calculated absorption (smoothed with a conservative linewidth of 15 meV [12,34], a value low enough to smooth numerical noise without dominating the inhomogeneous broadening) to the experimental data. An excellent agreement is obtained without adjusting any model parameter. The amplitude and shape of the excitonic peak and of the low-energy edge are well reproduced. For comparison, Fig. 1(c) also shows a calculation where alloy disorder is ignored: the corresponding excitonic peak is much too sharp. This confirms that Anderson localization dominates the inhomogeneous broadening in flat-band absorption spectra. The slight underestimation of α at high energy may be due to our two-band framework (e.g., the contribution from higher hole bands is missing).

III. LUMINESCENCE

Having addressed optical absorption, we turn to the more complex and important study of luminescence—more specifically luminescence dynamics, for which many-body effects can cause a departure from the conventional bimolecular radiative rate $G_r = Bn^2$ (with B the radiative coefficient and n the carrier density).

We study a series of QW samples similar to the previous sample, with varying QW thickness. Luminescence is measured without an applied bias—although optical excitation causes a photobias of approximately 2 V, leading to a band structure similar to that of an LED under electrical injection. This band profile causes a separation of electrons and holes compared to the flat-band case studied above, and hence a lower Coulomb interaction; nevertheless, Coulomb effects remain relevant, as will be shown.

The *p-i-n* epitaxial structure precludes artifacts from modulation doping [35] and carrier escape [36], thus enabling a proper measurement of carrier dynamics using an all-optical differential lifetime measurement [37]. In contrast to conventional large-signal measurements, this technique gives direct access to the lifetime and carrier density n over a wide range of excitation levels, without requiring assumptions on a recombination model. By combining this with a measurement of the sample's absolute internal quantum efficiency (IQE), we obtain the effective radiative coefficient $B(n) = G_r/n^2$ [38].

We measure B for a series of five samples spanning QW thicknesses between 2.5 and 4.5 nm, as shown in Fig. 2. These data show an intricate behavior. At high carrier density, B increases for most samples; as discussed in our previous work, this is simply due to screening of the polarization field by injected carriers [37]. Qualitatively, screening should be most pronounced for thicker samples (where the potential drop due to the polarization field is larger), as we do observe experimentally.

The behavior at low density, however, defies common expectation: instead of a plateau (characteristic of standard bimolecular recombination), B shows a clear carrier dependence, increasing up to tenfold at low density—this is most pronounced in thin QWs. The remainder of this Letter is dedicated to investigating this remarkable trend.

One may first wonder if carrier localization can alone cause the observed increase of B . We verify that this is not the case by computing the radiative rate for free carriers (i.e., carriers without Coulomb interaction) in a QW with alloy disorder. As shown as dashed lines in Fig. 2(a), a bimolecular rate is still predicted. This conclusion is unsurprising, as the bimolecular behavior is generally robust against the details of transition selection rules [39]. Furthermore, our calculations with disorder alone only lead to a small correction to B from the disorder-free case (see SM [30]): this is in line with other theoretical investigation [18–21], but does not reproduce the experimental order-of-magnitude increase in B , showing that disorder alone is insufficient to explain the data.

Instead, one must again consider many-body effects to account for the radiative dynamics. Studies in various material systems have shown how Coulomb interaction increases the radiative rate at low density [22,40–43].

We therefore extend the model to encompass luminescence. Highly accurate approaches exist for this task [44];

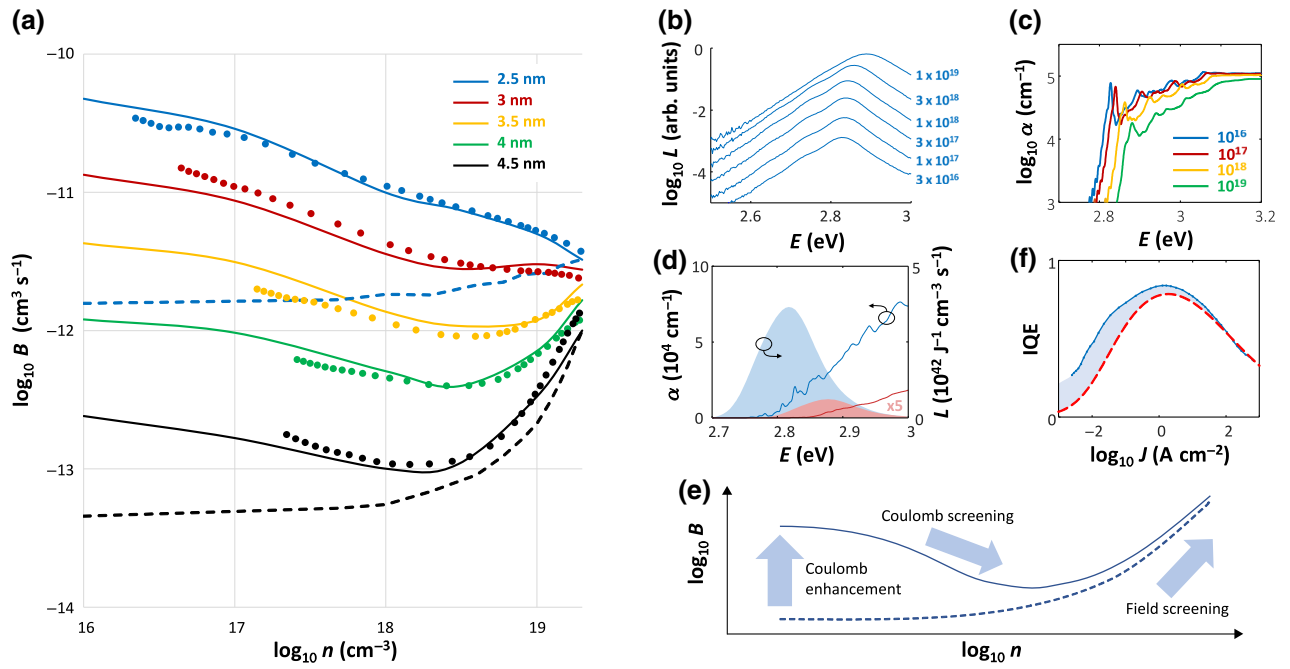


FIG. 2. Photoluminescence properties of (In,Ga)N QWs. (a) Effective radiative coefficient versus carrier density. Dots, experimental measurements, revealing a departure from bimolecular recombination. Dashed lines, model including disorder but ignoring Coulomb interaction, resulting in a bimolecular rate, i.e., a plateau at low density with an increase due to field screening at high density (shown only for the thinnest and thickest QWs). Solid lines, full model. (b) Experimental luminescence spectra L for a 3-nm QW, indicative of thermalized carrier distributions at all carrier densities (densities as labeled). (c) Modeled carrier-density-dependent absorption for one configuration of a 3-nm QW (densities as labeled). (d) Modeled absorption α (lines) and luminescence L (shaded shapes) for a 3-nm QW; blue and red, with and without Coulomb interaction. (e) Sketch of the trends observed in (a). (f) IQE of a 2.5-nm QW versus current density J . Solid line, measured IQE; dashed line, predicted IQE in the absence of Coulomb enhancement.

however, these are prohibitively complex for the present six-dimensional problem. Instead, as detailed hereafter, we proceed at the lowest order by deriving a carrier-dependent absorption spectrum, then transforming it into a luminescence spectrum (see SM [30] for further discussion).

The impact of carriers on absorption is included by computing a statically screened Coulomb potential: $V_{Cs} = V_C \exp(-\kappa\bar{r})$, with κ the Thomas-Fermi screening length (see details in SM [30]) [45]. This screened potential is used to compute the screened absorption spectrum, using the same procedure as before. Figure 2(c) illustrates results for a 3-nm QW. The Coulomb enhancement is maximal at low density, and is progressively screened until the free-carrier limit is reached at high density. Note that the enhancement is comprised of excitonic peaks and the Sommerfeld factor [45], although the distinction between bound states and continuum is not well defined in the presence of disorder.

To then obtain luminescence spectra, we make assumptions on the carrier populations. First, we assume that all the carriers exist as an electron-hole plasma, with no exciton population. This is well justified at room temperature considering Saha's equation (see SM [30]) [46,47]. Thus,

in this model, the luminescence enhancement is not due to the presence of an excitonic population, but solely to an increase of the JDOS by the Coulomb interaction—a distinction discussed in detail in Refs. [41] and [42]. Second, we assume that the carriers are in quasithermal equilibrium, and described by Fermi-Dirac populations. This assumption may not be obvious for holes in the presence of Anderson localization; however, the following considerations justify it: (i) our free-carrier computations confirm that only the lowest-energy hole states are localized, while populated higher-energy hole states extend laterally and enable population thermalization (see SM [30]); and (ii) experimental room-temperature luminescence spectra indeed display a thermalized tail, independent of carrier density [Fig. 2(b)].

Under these assumptions, the densities of states for free electrons and holes are derived by computing eigenstates of the respective three-dimensional Poisson-Schrodinger equations. Several thousand states are computed, enough to generate accurate densities of states and the corresponding Fermi-Dirac distributions $f_{c,v}$.

Absorption and luminescence are related by the Kubo-Martin-Schwinger (KMS) relationship [48–51]. Here we use a generalization of this relationship, valid in disordered

systems (see SM [30]):

$$L(E) = \frac{E^2 n_r^2}{\pi^2 c^2 \hbar^3} \alpha \langle f_c (1 - f_v) \rangle, \quad (2)$$

where L is the luminescence spectrum, E the emission energy, n_r the refractive index, α the absorption with Coulomb enhancement, and $\langle \cdot \rangle$ denotes an average over all pairs of electron-hole states with transition energy E , weighed by their wave function overlap. In the non-Coulomb-interacting case, Eq. (2) exactly predicts L . To compute luminescence with many-body effects, we apply this relationship with carrier distributions given by their free densities of state, but replacing the free-carrier absorption with the Coulomb-interacting one [22]. This approximation is accurate at high enough temperature [41]. The resulting Coulomb enhancement of L is illustrated in Fig. 2(d).

Finally, we obtain the radiative coefficient with many-body enhancement as $B = \int L(E) dE / n^2$. The resulting B coefficients are shown on Fig. 2(a). To best match the experimental data, the modeled QW thickness was adjusted by +0.5 nm for all samples (a correction within the experimental uncertainty on the QW thickness). The resulting predictions are in excellent agreement with the experimental data, reproducing the relative variation of B with QW thickness and its carrier dependence.

Therefore, the behavior of the radiative rate at low current can be understood as follows. By increasing α , many-body interaction leads to an enhanced radiative rate; this appears as the difference between the full and dashed curves in Fig. 2(a). This interaction is most pronounced for thin QWs (where the electron and hole wave functions are closely confined) and weaker for thick QWs (where the wave functions are separated). The enhancement is modulated by in-plane carrier localization, and is further screened by carriers, leading to a reduction of B towards its noninteracting value with carrier density. In addition, at high density ($n > 10^{18} \text{ cm}^{-3}$), polarization-field screening occurs and B increases, especially in the thicker samples. The relative contribution of screened Coulomb interaction and field screening to B depends on the QW thickness; the plateau in B displayed by some sample corresponds to the regime where Coulomb enhancement becomes small. Figure 2(e) illustrates these considerations.

Importantly, this enhancement can have a profound impact on the efficiency of real-world LED devices. For instance, at a moderate carrier density 10^{17} cm^{-3} , Coulomb enhancement increases the radiative rate by an order of magnitude in thin QWs. As shown in Fig. 2(f), this causes a substantial improvement in low-current efficiency, where radiative emission competes with Shockley-Read-Hall recombinations. Low-current operation is uncommon in lighting applications, but should be of particular interest in future devices such as micro-LED displays. In

this case, our findings indicate that the radiative rate can be boosted by employing very thin QWs to maximize Coulomb enhancement. Incidentally, Fig. 2(f) illustrates that Coulomb enhancement is encoded in the low-current shape of the IQE curve and its departure from a conventional ABC recombination model.

IV. CONCLUSIONS

In summary, we show that strongly disordered (In,Ga)N quantum wells are a remarkable system with pronounced localization and many-body effects directly observed in room-temperature optical properties. We introduce a state-of-the-art nonperturbative model, which treats alloy disorder and Coulomb interaction on equal footing, accurately and efficiently tackling this challenging numerical problem. The model confirms that the interplay between localization and Coulomb interaction dominates the optical properties of (In,Ga)N quantum emitters, making them an ideal testbed for future explorations of these complex optical effects, and shedding new insight into the efficiency of modern LEDs.

ACKNOWLEDGMENTS

A.D. would like to acknowledge Claude Weisbuch for stimulating conversations on the topic of localization.

-
- [1] C. Weisbuch, R. Dingle, A. C. Gossard, and W. Wiegmann, Optical characterization of interface disorder in GaAs-Ga_{1-x}Al_xAs multi-quantum well structures, *Solid State Commun.* **38**, 709 (1981).
 - [2] H. Wang, M. Jiang, and D. G. Steel, Measurement of Phonon-assisted Migration of Localized Excitons in GaAs/AlGaAs Multiple-quantum-well Structures, *Phys. Rev. Lett.* **65**, 1255 (1990).
 - [3] A. Zrenner, L. V. Butov, M. Hagn, G. Abstreiter, G. Bohm, and G. Weimann, Quantum Dots Formed by Interface Fluctuations in AlAs/GaAs Coupled Quantum Well Structures, *Phys. Rev. Lett.* **72**, 3382 (1994).
 - [4] K. Brunner, G. Abstreiter, G. Bohm, G. Trankle, and G. Weimann, Sharp-line Photoluminescence and Two-photon Absorption of Zero-dimensional Biexcitons in a GaAs/AlGaAs Structure, *Phys. Rev. Lett.* **73**, 1138 (1994).
 - [5] D. Gammon, E. S. Snow, B. V. Shanabrook, D. S. Katzer, and D. Park, Fine Structure Splitting in the Optical Spectra of Single GaAs Quantum Dots, *Phys. Rev. Lett.* **76**, 3005 (1996).
 - [6] V. Savona, S. Haacke, and B. Deveaud, Optical Signatures of Energy-level Statistics in a Disordered Quantum System, *Phys. Rev. Lett.* **84**, 183 (2000).
 - [7] F. Intonti, V. Emiliani, C. Lienau, T. Elsaesser, V. Savona, E. Runge, R. Zimmermann, R. Noetzel, and K. H. Ploog, Quantum Mechanical Repulsion of Exciton Levels in a Disordered Quantum Well, *Phys. Rev. Lett.* **87**, 076801 (2001).

- [8] W. Langbein, E. Runge, V. Savona, and R. Zimmermann, Enhanced Resonant Backscattering of Excitons in Disordered Quantum Wells, *Phys. Rev. Lett.* **89**, 157401 (2002).
- [9] Y. Yayon, A. Esser, M. Rappaport, V. Umansky, H. Shtrikman, and I. Bar-Joseph, Long-range Spatial Correlations in the Exciton Energy Distribution in GaAs/AlGaAs Quantum Wells, *Phys. Rev. Lett.* **89**, 157402 (2002).
- [10] S. F. Chichibu, A. Uedono, T. Onuma, B. A. Haskell, A. Chakraborty, T. Koyama, P. T. Fini, S. Keller, S. P. Denbaars, J. S. Speck, U. K. Mishra, S. Nakamura, S. Yamaguchi, S. Kamiyama, H. Amano, I. Akasaki, J. Han, and T. Sota, Origin of defect-insensitive emission probability in In-containing (Al,In,Ga)N alloy semiconductors, *Nat. Mater.* **5**, 810 (2006).
- [11] M. Piccardo, C.-K. Li, Y.-R. Wu, J. S. Speck, B. Bonef, R. M. Farrell, M. Filoche, L. Martinelli, J. Peretti, and C. Weisbuch, Localization landscape theory of disorder in semiconductors. II. Urbach tails of disordered quantum well layers, *Phys. Rev. B* **95**, 144205 (2017).
- [12] W. Hahn, J. M. Lentali, P. Polovodov, N. Young, S. Nakamura, J. S. Speck, C. Weisbuch, M. Filoche, Y. R. Wu, and M. Piccardo, Evidence of nanoscale Anderson localization induced by intrinsic compositional disorder in InGaN/GaN quantum wells by scanning tunneling luminescence spectroscopy, *Phys. Rev. B* **98**, 045305 (2018).
- [13] W. E. Blenkhorn, S. Schulz, D. S. P. Tanner, R. A. Oliver, M. J. Kappers, C. J. Humphreys, and P. Dawson, Resonant photoluminescence studies of carrier localisation in c-plane InGaN/GaN quantum well structures, *J. Phys.: Condens. Matter* **30**, 175303 (2018).
- [14] S. John, C. Soukoulis, M. H. Cohen, and E. N. Economou, Theory of Electron Band Tails and the Urbach Optical-absorption Edge, *Phys. Rev. Lett.* **57**, 1777 (1986).
- [15] S. Schulz, D. P. Tanner, E. P. O'Reilly, M. A. Caro, T. L. Martin, P. A. J. Bagot, M. P. Moody, F. Tang, J. T. Griffiths, and F. Oehler, Structural, electronic, and optical properties of m-plane InGaN/GaN quantum wells: Insights from experiment and atomistic theory, *Phys. Rev. B* **92**, 235419 (2015).
- [16] W. Liu, R. Butte, A. Dussaigne, N. Grandjean, B. Deveaud, and G. Jacopin, Carrier-density-dependent recombination dynamics of excitons and electron-hole plasma in m-plane InGaN/GaN quantum wells, *Phys. Rev. B* **94**, 195411 (2016).
- [17] D. Watson-Parris, M. J. Godfrey, P. Dawson, R. A. Oliver, M. J. Galtrey, M. J. Kappers, and C. J. Humphreys, Carrier localization mechanisms in $\text{In}_x\text{Ga}_{1-x}\text{N}/\text{GaN}$ quantum wells, *Phys. Rev. B* **83**, 115321 (2011).
- [18] S. Schulz, M. A. Caro, C. Coughlan, and E. P. O'Reilly, Atomistic analysis of the impact of alloy and well-width fluctuations on the electronic and optical properties of InGaN/GaN quantum wells, *Phys. Rev. B* **91**, 035439 (2015).
- [19] M. Auf der Maur, A. Pecchia, G. Penazzi, W. Rodrigues, and A. Di Carlo, Efficiency Drop in Green InGaN/GaN Light Emitting Diodes: The Role of Random Alloy Fluctuations, *Phys. Rev. Lett.* **116**, 027401 (2016).
- [20] C.-K. Li, M. Piccardo, L.-S. Lu, S. Mayboroda, L. Martinelli, J. Peretti, J. S. Speck, C. Weisbuch, M. Filoche, and Y.-R. Wu, Localization landscape theory of disorder in semiconductors. III. Application to carrier transport and recombination in light emitting diodes, *Phys. Rev. B* **95**, 144206 (2017).
- [21] C. M. Jones, C.-H. Teng, Q. Yan, P.-C. Ku, and E. Kioupakis, Impact of carrier localization on recombination in InGaN quantum wells and the efficiency of nitride light-emitting diodes: Insights from theory and numerical simulations, *Appl. Phys. Lett.* **111**, 113501 (2017).
- [22] W. Chow, M. Kira, and S. W. Koch, Microscopic theory of optical nonlinearities and spontaneous emission lifetime in group-II nitride quantum wells, *Phys. Rev. B* **60**, 1947 (1999).
- [23] J. Hader, J. V. Moloney, A. Thranhardt, and S. W. Koch, in *Nitride Semiconductor Devices*, edited by J. Piprek (Wiley-VCH, Weinheim, 2007), Chap. 7.
- [24] D. S. P. Tanner, J. M. McMahon, and S. Schulz, Interface Roughness, Carrier Localization, and Wave Function Overlap in C-plane (In, Ga)N/GaN Quantum Wells: Interplay of Well Width, Alloy Microstructure, Structural Inhomogeneities, and Coulomb Effects, *Phys. Rev. Appl.* **10**, 034027 (2018).
- [25] R. Dingle, D. D. Sell, S. E. Stokowski, and M. Ilegems, Absorption, reflectance, and luminescence of GaN epitaxial layers, *Phys. Rev. B* **4**, 1211 (1971).
- [26] R. T. Collins, K. V. Klitzing, and K. Ploog, Photocurrent spectroscopy of GaAs/Al_xGa_{1-x}As quantum wells in an electric field, *Phys. Rev. B* **33**, 4378 (1986).
- [27] A. David and M. J. Grundmann, Influence of polarization fields on carrier lifetime and recombination rates in InGaN-based light-emitting diodes, *Appl. Phys. Lett.* **97**, 033501 (2010).
- [28] S. Glutsch, D. S. Chemla, and F. Bechstedt, Numerical calculation of the optical absorption in semiconductor quantum structures, *Phys. Rev. B* **54**, 11592 (1996).
- [29] S. Glutsch, *Excitons in Low-dimensional Semiconductors: Theory Numerical Methods Applications* (Springer, Berlin, 2004), Vol. 141.
- [30] See Supplemental Material at <http://link.aps.org/supplemental/10.1103/PhysRevApplied.12.044059> for details of the numerical model. The SM makes reference to Refs. [52–58].
- [31] A. Gordon, C. Jirauschek, and F. X. Kartner, Numerical solver of the time-dependent Schrodinger equation with Coulomb singularities, *Phys. Rev. A* **73**, 042505 (2006).
- [32] In contrast, the ground-state scheme requires a preliminary calculation of the ground state for the one-dimensional excitonic problem, which only exists below the Mott density.
- [33] E. F. Schubert and W. T. Tsang, Photoluminescence line shape of excitons in alloy semiconductors, *Phys. Rev. B* **34**, 2991 (1986).
- [34] M. J. Holmes, K. Choi, S. Kako, M. Arita, and Y. Arakawa, Room-temperature triggered single photon emission from a III-nitride site-controlled nanowire quantum dot, *Nano Lett.* **14**, 982 (2014).
- [35] T. Langer, A. Chernikov, D. Kalincev, M. Gerhard, H. Bremers, U. Rossow, M. Koch, and A. Hangleiter, Room temperature excitonic recombination in GaInN/GaN

- quantum wells, *Appl. Phys. Lett.* **103**, 202106 (2013).
- [36] A. David, C. A. Hurni, N. G. Young, and M. D. Craven, Carrier dynamics and Coulomb-enhanced capture in III-nitride quantum heterostructures, *Appl. Phys. Lett.* **109**, 033504 (2016).
- [37] A. David, N. G. Young, C. A. Hurni, and M. D. Craven, All-optical measurements of carrier dynamics in bulk-GaN LEDs: Beyond the ABC approximation, *Appl. Phys. Lett.* **110**, 253504 (2017).
- [38] A. David and M. J. Grundmann, Droop in InGaN light-emitting diodes: A differential carrier lifetime analysis, *Appl. Phys. Lett.* **96**, 103504 (2010).
- [39] G. Lasher and F. Stern, Spontaneous and stimulated recombination radiation in semiconductors, *Phys. Rev.* **133**, A553 (1964).
- [40] H. Schlangenotto, H. Maeder, and W. Gerlach, Temperature dependence of the radiative recombination coefficient in silicon, *Phys. Status Solidi (a)* **21**, 357 (1974).
- [41] S. Chatterjee, C. Ell, S. Mosor, G. Khitrova, H. M. Gibbs, W. Hoyer, M. Kira, S. W. Koch, J. P. Prineas, and H. Stolz, Excitonic Photoluminescence in Semiconductor Quantum Wells: Plasma versus Excitons, *Phys. Rev. Lett.* **92**, 067402 (2004).
- [42] S. W. Koch, M. Kira, G. Khitrova, and H. M. Gibbs, Semiconductor excitons in new light, *Nat. Mater.* **5**, 523 (2006).
- [43] P. P. Altermatt, F. Geelhaar, T. Trupke, X. Dai, A. Neisser, and E. Daub, Injection dependence of spontaneous radiative recombination in crystalline silicon: Experimental verification and theoretical analysis, *Appl. Phys. Lett.* **88**, 261901 (2006).
- [44] M. Kira, F. Jahnke, and S. W. Koch, Microscopic Theory of Excitonic Signatures in Semiconductor Photoluminescence, *Phys. Rev. Lett.* **81**, 3263 (1998).
- [45] H. Haug and S. W. Koch, *Quantum Theory of the Optical and Electronic Properties of Semiconductors* (World Scientific Publishing Company, Singapore, 2009), 5th ed.
- [46] D. S. Chemla, D. Miller, P. Smith, A. Gossard, and W. Wiegmann, Room temperature excitonic nonlinear absorption and refraction in GaAs/AlGaAs multiple quantum well structures, *IEEE J. Quantum Electron.* **20**, 265 (1984).
- [47] D. Snoke, Predicting the ionization threshold for carriers in excited semiconductors, *Solid State Commun.* **146**, 73 (2008).
- [48] W. Van Roosbroeck and W. Shockley, Photon-radiative recombination of electrons and holes in germanium, *Phys. Rev.* **94**, 1558 (1954).
- [49] R. Kubo, Statistical-mechanical theory of irreversible processes. I. General theory and simple applications to magnetic and conduction problems, *J. Phys. Soc. Jpn.* **12**, 570 (1957).
- [50] P. C. Martin and J. Schwinger, Theory of many-particle systems. I, *Phys. Rev.* **115**, 1342 (1959).
- [51] R. Bhattacharya, B. Pal, and B. Bansal, On conversion of luminescence into absorption and the van roosbroeck-shockley relation, *Appl. Phys. Lett.* **100**, 222103 (2012).
- [52] I. Vurgaftman and J. R. Meyer, Band parameters for nitrogen-containing semiconductors, *J. Appl. Phys.* **94**, 3675 (2003).
- [53] P. G. Moses and C. G. Van de Walle, Band bowing and band alignment in InGaN alloys, *Appl. Phys. Lett.* **96**, 021908 (2010).
- [54] C. A. Hurni, H. Kroemer, U. K. Mishra, and J. S. Speck, Capacitance-voltage profiling on polar III-nitride heterostructures, *J. Appl. Phys.* **112**, 083704 (2012).
- [55] U. M. E. Christmas, A. D. Andreev, and D. A. Faux, Calculation of electric field and optical transitions in InGaN/GaN quantum wells, *J. Appl. Phys.* **98**, 073522 (2005).
- [56] S. Schulz, A. Berube, and E. P. O. Reilly, Polarization fields in nitride-based quantum dots grown on nonpolar substrates, *Phys. Rev. B* **79**, 081401 (2009).
- [57] M. L. Zambrano and J. C. Arce, Stark-resonance densities of states, eigenfunctions, and lifetimes for electrons in GaAs/(Al, Ga) As quantum wells under strong electric fields: An optical-potential wave-packet propagation method, *Phys. Rev. B* **66**, 155340 (2002).
- [58] L. Banyai and S. W. Koch, A simple theory for the effects of plasma screening on the optical spectra of highly excited semiconductors, *Z. Phys. B: Condens. Matter* **63**, 283 (1986).